Charge Transfer

DOI: 10.1002/anie.201002881

Water-Switching of Spin Transitions Induced by Metal-to-Metal Charge Transfer in a Microporous Framework

*Tao Liu, Yan-Juan Zhang, Shinji Kanegawa, and Osamu Sato**

The design and synthesis of tunable molecular magnets, the magnetic properties of which are sensitive to external stimuli such as light, heat, pressure, and guest molecules, are of current interest.[1–3] Advances in porous magnets have been made by combining porosity with spin crossover or long-range magnetic ordering, such as bidirectional chemo-switching of spin crossover,[2] reversible ferromagnetic/antiferromagnetic transformation,[3] and critical-temperature shifts.[4] Moreover, one of the most effective ways to tune the magnetic properties of molecular magnets is through light- or heat-induced metal-to-metal charge transfer (MMCT),[5] because the charge-transfer process involves concomitant spin-state changes at the metal centers and is very sensitive to structure transformations.[6] Achim et al. demonstrated that solvent content plays an important role in determining the temperature range in which MMCT occurs in pentanuclear Co_3Fe_2 complexes.[6c] Beuzen et al. showed that MMCT and photomagnetic properties can be controlled by tuning the ratio of cyanide and water ligands of the cobalt coordination sphere of CoFe Prussian blue analogues.[6d] We aimed at combining porosity and MMCT to realize guest-tunable MMCT through guest adsorption, because host–guest interactions have both profound and subtle effects on the redox potential of redox pairs.[7] Although many examples involving MMCT have been documented,[8] direct coupling of porosity and charge transfer is still undeveloped.

Herein we report water-switchable MMCT by dehydration and rehydration in a microporous framework. Pentahydrate $[Fe(Tp)(CN)_3]_2Co(bpe)\cdot 5H_2O$ (**1**·5 H_2O; Tp = hydrotris(pyrazolyl)borate; bpe = 1,2-bis(4-pyridyl)ethane) shows reversible light- and temperature-induced charge transfer between $Fe^{III}_{LS}(\mu\text{-}CN)Co^{II}_{HS}$ (HS = high spin, LS = low spin) and $Fe^{II}_{LS}(\mu\text{-}CN)Co^{III}_{LS}$ redox pairs, whereas we observed no MMCT in dehydrated **1**. The transformation between **1**·5 H_2O and **1**, as well as their magnetic properties, is reversible by de- and rehydration.

We synthesized **1**·5 H_2O by reaction of $Li[Fe(Tp)(CN)_3]$, $Co(NO_3)_2\cdot 6H_2O$, and 1,2-bis(4-pyridyl)ethane in water. Single-crystal XRD analysis revealed that **1**·5 H_2O crystallizes in monoclinic space group $P2_1/c$. The crystal structure consists of neutral bimetallic $[Fe(Tp)(CN)_3]_2Co(bpe)$ layers with uncoordinated water molecules between the layers (Figure 1 and Figure S1 of the Supporting Information). Within the neutral layer, each $[Fe(Tp)(CN)_3]^-$ entity acts as a bidentate

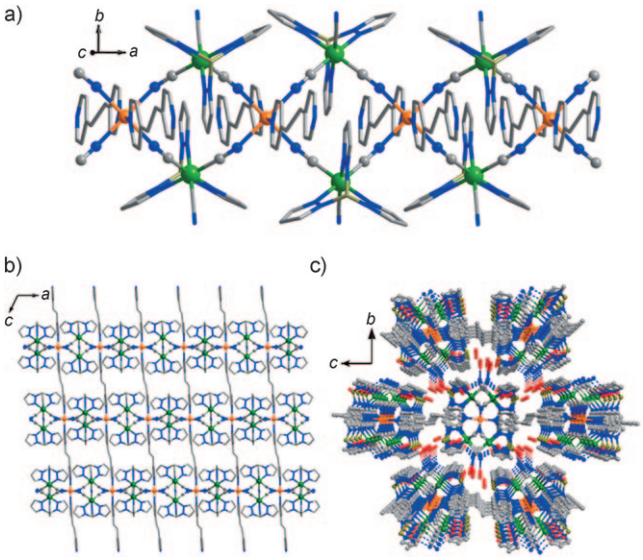

Figure 1. a) Side view of the double zigzag chain in **1**·5 H_2O along the *c* axis. b) Side view of the layer structure in **1**·5 H_2O along the *b* axis. c) Packing structure of **1**·5 H_2O along the *a* axis. The dashed lines represent hydrogen bonds between uncoordinated water molecules and terminal cyanide nitrogen atoms. Fe green, Co orange, N blue, O red, C gray, and B dark yellow.

ligand toward two Co^{II} ions through two of its three cyanide groups in *cis* positions, and each Co^{II} is coordinated by four nitrogen atoms from CN^- bridges to afford bimetallic double-zigzag chains that run parallel to the *a* axis (Figure 1 a). The chain structure is similar to other reported $Fe^{III}_2Co^{II}$ double-zigzag chains.[9] The square units exhibit two orientations of their mean planes ($Fe^{III}_2Co^{II}_2$), the dihedral angle of which is hereafter denoted ϕ. The chains are further linked by bpe ligands along the apical direction of the cobalt centers, affording a layer framework (Figure 1 b). The $[Fe(Tp)(CN)_3]_2Co(bpe)$ layers are arranged in the *ac* plane and stacked along the *b* axis (Figure 1 c) through hydrogen bonding between pyrazolyl carbon atoms and terminal cyanide nitrogen atoms (C···N 3.19–3.52 Å). Hydrogen bonds between uncoordinated water molecules and terminal cyanide nitrogen atoms (O···N 2.91–3.14 Å; Figure 1 c). The crystal structure comprises two unique iron centers and one unique cobalt center. Two nitrogen atoms from bpe and four cyanide carbon atoms are coordinated to each iron center,

[*] Dr. T. Liu, Dr. Y.-J. Zhang, Dr. S. Kanegawa, Prof. O. Sato
Institute for Materials Chemistry and Engineering
Kyushu University
6-1 Kasuga, 816-8580, Fukuoka (Japan)
Fax: (+81) 92-583-7787
E-mail: sato@cm.kyushu-u.ac.jp

Supporting information for this article is available on the WWW under http://dx.doi.org/10.1002/anie.201002881.

and each cobalt center is located in the elongated N_6 octahedral environment with four short equatorial Co–N distances and two longer apical Co–N distances. At 223 K, the $Co–N_{equatorial}$ and $Co-N_{apical}$ bond lengths are 2.116–2.122 and 2.148–2.152 Å, respectively. The Fe–C bond lengths are 1.893–1.912 and 1.910–1.925 Å for Fe1 and Fe2, respectively, and the Fe–N bond lengths are 1.966–1.977 and 1.968–1.984 Å for Fe1 and Fe2, respectively. Valence sum bond analysis and charge compensation indicated that the cobalt centers are $Co^{II}{}_{HS}$, while the iron centers are $Fe^{III}{}_{LS}$, and $Fe^{III}{}_{LS}$(μ-CN)$Co^{II}{}_{HS}$ linkages are formed.[8,10] The ϕ value is 52°.

When crystals of **1**·5 H_2O were slowly cooled from 223 to 123 K, their color changed from red to dark green. At 123 K, $Co–N_{equatorial}$ and $Co–N_{apical}$ bond lengths were 1.908–1.930 and 1.986–2.006 Å, respectively, which are significantly shorter than expected for $Co^{II}{}_{HS}$ (ca. 2.1 Å) but slightly longer than expected for $Co^{III}{}_{LS}$ (ca. 1.9 Å).[8,10] The Fe–C bond lengths are 1.925–1.951 Å and 1.885–1.898 Å for Fe1 and Fe2, respectively, and the Fe–N bond lengths 1.959–2.000 and 2.032–2.038 Å for Fe1 and Fe2, respectively. The ϕ value of 49° suggests that the neighboring square units rotated by approximately 3° with respect to each other. These temperature-dependent structural variations in crystals of **1**·5 H_2O suggested that intramolecular charge transfer partially converted $Fe^{III}{}_{LS}$(μ-CN)$Co^{II}{}_{HS}$ units to $Fe^{II}{}_{LS}$(μ-CN)$Co^{III}{}_{LS}$ units and that Fe^{II}, Fe^{III}, Co^{II}, and Co^{III} were randomly arranged.

We obtained single crystals of **1** by pumping crystals of **1**·5 H_2O to vacuum at room temperature. Thermogravimetric analysis (TGA) of **1**·5 H_2O showed a weight loss of 9.1% in the temperature range 30–80 °C, corresponding to loss of five water molecules (8.8%; Figure S2, Supporting Information). After this weight loss, a long plateau was observed up to the decomposition temperature of about 220 °C. Dehydrated **1** crystallized in space group C_2/c. The framework of **1** is similar to that of **1**·5 H_2O, but lacks the hydrogen bonds between uncoordinated water molecules and terminal cyanide nitrogen atoms. From the packing diagram, one-dimensional channels along the c direction are evident (Figure S3, Supporting Information). The channel size is 1.2 × 3.1 Å (excluding the van der Waals radii of the surface atoms) and the void space (calculated with PLATON)[11] is 22.8%. The crystal structure contains of one unique iron center and one unique cobalt center. At 223 K, the $Co–N_{equatorial}$ and $Co–N_{apical}$ bond lengths are 2.114–2.118 and 2.172 Å, respectively. At 123 K, the $Co–N_{equatorial}$ and $Co–N_{apical}$ bond lengths are 2.108–2.113 Å and 2.169 Å, respectively. Structural parameters indicated that the cobalt centers are $Co^{II}{}_{HS}$ at both temperatures,[8,10] and $Fe^{III}{}_{LS}$(μ-CN)$Co^{II}{}_{HS}$ linkages are formed according to charge compensation. The ϕ value is 52° at both 223 and 123 K, the same as in **1**·5 H_2O at 223 K.

Additional support for the water-switchable MMCT hypothesis can be found in temperature-dependent IR spectroscopic studies on **1**·5 H_2O and **1** between 300 and 77 K (Figure 2). For **1**·5 H_2O, we observed two ν_{CN} bands (2126 and 2152 cm^{-1}) at 300 K, corresponding to the free ν_{CN} mode of $[Fe^{III}Tp(CN)_3]^-$ and the bridging ν_{CN} mode of $Fe^{III}{}_{LS}$(μ-CN)$Co^{II}{}_{HS}$ linkages, respectively. With decreasing temperature, new ν_{CN} bands were observed, which were attributed to the free ν_{CN} mode (2060 cm^{-1}) of

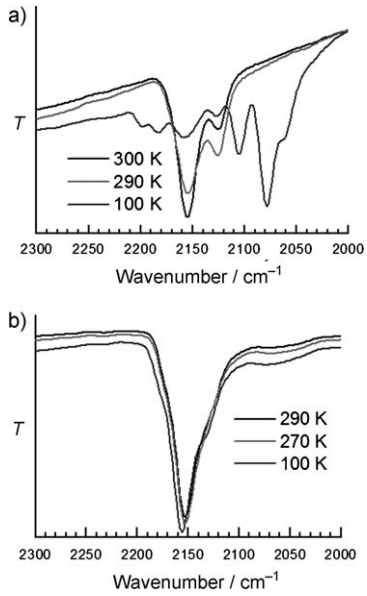

Figure 2. a) Infrared spectra of **1**·5 H_2O on cooling (300 K, 100 K) and heating (290 K). b) Infrared spectra of **1** on cooling (290 K, 100 K) and heating (270 K).

$[Fe^{II}Tp(CN)_3]^{2-}$ and the bridging ν_{CN} modes of $Fe^{II}{}_{LS}$(μ-CN)$Co^{II}{}_{HS}$ (2077 cm^{-1}), $Fe^{II}{}_{LS}$(μ-CN)$Co^{III}{}_{LS}$ (2105 cm^{-1}), and $Fe^{III}{}_{LS}$(μ-CN)$Co^{III}{}_{LS}$ (2183 and 2197 cm^{-1}) linkages.[8,12] These IR results suggest that Fe^{III} and Co^{II} are only partially involved in MMCT. Moreover, these temperature-induced changes in the IR spectra of **1**·5 H_2O were completely reversible on warming the samples. These IR results are consistent with induction of reversible MMCT. For **1**, we observed two cyano stretching bands in the entire temperature range, corresponding to the free ν_{CN} mode of $[Fe^{III}Tp(CN)_3]^-$ (2130 cm^{-1}) and the bridging ν_{CN} mode of $Fe^{III}{}_{LS}$(μ-CN)$Co^{II}{}_{HS}$ linkages (2153 cm^{-1}), that is, no MMCT occurred.

Magnetic measurements verified water-switchable MMCT between **1**·5 H_2O and **1**. For **1**·5 H_2O, the χT value remained nearly constant between 300 and 220 K (Figure 3). However, slowly decreasing the temperature (2.0 K min^{-1}) from 220 to 100 K afforded a decrease in χT, which reached 1.90 $cm^3 mol^{-1} K$ at 120 K (Figure 3, inset). On the other hand,

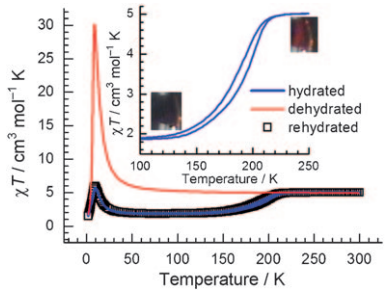

Figure 3. Temperature-dependent susceptibilities of **1** (red line), **1**·5 H_2O (blue line), and rehydrated sample (□). Inset: thermal hysteresis in χT versus T of **1**·5 H_2O and crystal colors of the HT and LT phases.

on heating (2.0 K min^{-1}), the χT values increased and returned to the initial value with a small thermal hysteresis loop. Such magnetic behavior confirmed a reversible charge-transfer process that involves transformation between the high-temperature (HT) phase with Fe^{III}_{LS} ($S=1/2$) and Co^{II}_{HS} ($S=3/2$) ions and the low-temperature (LT) phase with diamagnetic Fe^{II}_{LS} ($S=0$) and Co^{III}_{LS} ($S=0$) centers. According to the χT values, about two-thirds of Co^{II}_{HS} changed to Co^{III}_{LS} from the HT phase to the LT phase. Hence, the transformation could be expressed by $\{[Fe^{III}Tp(CN)_3]_2Co(bpe)\}\cdot 5H_2O \rightleftarrows \{[Fe^{III}Tp(CN)_3]_{4/3}[Fe^{II}Tp(CN)_3]_{2/3}Co^{III}_{2/3}Co^{II}_{1/3}(bpe)\}\cdot 5H_2O$. As the temperature further decreased from 120 K, the χT values remained nearly constant until 50 K and then increased to a maximum at 9.5 K before decreasing further.

We investigated the photoeffect of the LT phase of **1**·5 H_2O to probe the possibility of a photoinduced transformation from diamagnetic $Fe^{II}_{LS}(\mu\text{-}CN)Co^{III}_{LS}$ to metastable paramagnetic $Fe^{III}_{LS}(\mu\text{-}CN)Co^{II}_{LS}$ units. On light irradiation at 5 K for more than 12 h, a significant increase of the χT value occurred (Figure 4 and Figure S4 of the Supporting Information). On heating, the χT value first increased steeply to a sharp maximum of 14.4 cm^3 mol^{-1} K at 9.5 K, then decreased gradually, and, around 100 K, overlapped with the plots of the χT value before photoirradiation. The photoinduced magnetization relaxed to the initial value on thermal treatment up to 150 K, that is, the magnetization could be increased by irradiation with light and recovered by thermal treatment.[13]

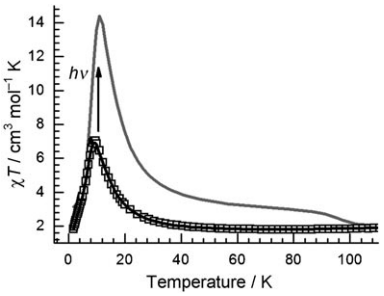

Figure 4. Temperature-dependent susceptibility of **1**·5 H_2O before irradiation (black line), after irradiation (gray line), and after thermal treatment up to 150 K (□).

For **1**, the χT value was 5.06 cm^3 mol^{-1} K per Fe_2Co unit at room temperature, which corresponds to the presence of one Co^{II}_{HS} and two Fe^{III}_{LS} with significant orbital contributions.[8,9] On cooling, the χT values increased with increasing rapidity, and reached a very sharp maxima of 30.3 cm^3 mol^{-1} K at 7.5 K, which indicates ferromagnetic interactions between Fe^{III} and Co^{II} (Figure 3). Then, the χT value rapidly decreased because of interchain antiferromagnetic interactions.

The transformation between **1** and **1**·5 H_2O involves changes in the switching of hydrogen bonds between uncoordinated water molecules and terminal cyanide nitrogen atoms. Such hydrogen bonds may play an important role in MMCT because hydrogen bonds can significantly tune redox potential, as reported for the non-heme Fe site of superoxide dismutase and quinone molecules.[14,15] Formation of hydrogen bonds has been reported to shift the redox potential of quinone molecules in the positive direction, while their disruption shifts the redox potential toward the negative.[7,15] In our study, **1**·5 H_2O displayed MMCT and $Fe^{II}_{LS}(\mu\text{-}CN)Co^{III}_{LS}$ pairs were stable at low temperatures. When the hydrogen bonds between uncoordinated water molecules and terminal cyanide nitrogen atoms were removed, the redox potential of Fe^{II}_{LS} shifted to negative potential, destabilizing the $Fe^{II}_{LS}(\mu\text{-}CN)Co^{III}_{LS}$ pairs and stabilizing the $Fe^{III}_{LS}(\mu\text{-}CN)Co^{II}_{HS}$ pairs. Therefore, dehydrated **1** did not demonstrate MMCT. When placed in water overnight or in water vapor for more than one week, reversible transformation of **1** into **1**·5 H_2O occurred, as evidenced by single-crystal XRD, C,H,N analysis, and TGA (Figure S2, Supporting Information). Since the transformation is accompanied by recovery of the heat-induced MMCT (Figure 3), water-switchable MMCT is confirmed.

In conclusion, we have synthesized the microporous compound $[Fe(Tp)(CN)_3]_2Co(bpe)$, in which heat- and light-induced MMCT could be reversibly switched through dehydration and rehydration. It should be interesting to study the effects of other guest molecules on MMCT, and endeavors to this end are in progress.

Experimental Section

Synthesis of **1**·5 H_2O: A solution of of $Li[Fe(Tp)(CN)_3]$[16] (0.1 mmol) in water (6.0 mL) was placed at the bottom of one side of an H-shaped tube, and a solution of of $Co(NO_3)_2\cdot 6H_2O$ (0.05 mmol) and 1,2-bis(4-pyridyl)ethane (0.05 mmol) in water (6.0 mL) in the other. 6.0 mL of water was layered on the solutions on both sides to provide a diffusion pathway. Crystallization took several weeks and gave crystals in a yield of 80 % based on $Co(NO_3)_2\cdot 6H_2O$. C,H,N analysis (%) calcd for $C_{36}H_{42}N_{20}O_5B_2CoFe_2$: C 42.10, H 4.12, N 27.27; found: C 41.74, H 4.07, N 26.85.

1 was obtained by continuously pumping crystals of **1**·5 H_2O to vacuum at room temperature for 3 h or by slowly heating crystals of **1**·5 H_2O to 100 °C under air. C,H,N analysis (%) calcd for $C_{36}H_{32}N_{20}B_2CoFe_2$: C 46.15, H 3.44, N 29.90; found: C 46.46, H 3.75, N 30.28. When placed in water overnight or in water vapor for more than one week, reversible transformation of **1** into **1**·5 H_2O occurred. C,H,N analysis (%) for rehydrated sample, calcd for $C_{36}H_{42}N_{20}O_5B_2CoFe_2$: C 42.10, H 4.12, N 27.27; found: C 41.90, H 3.96, N 26.81.

Received: May 12, 2010
Revised: July 17, 2010
Published online: October 4, 2010

Keywords: charge transfer · cobalt · iron · magnetic properties · microporous materials

[1] a) O. Sato, J. Tao, Y.-Z. Zhang, *Angew. Chem.* **2007**, *119*, 2200–2236; *Angew. Chem. Int. Ed.* **2007**, *46*, 2152–2187; b) M. B. Duriska, S. M. Neville, B. Moubaraki, J. D. Cashion, G. J. Halder, K. W. Chapman, C. Balde, J.-F. Létard, K. S. Murray, C. J. Kepert, S. R. Batten, *Angew. Chem.* **2009**, *121*, 2587–2590; *Angew. Chem. Int. Ed.* **2009**, *48*, 2549–2552; c) E. Coronado, M. C. Giménez-López, G. Levchenko, F. M. Romero, V. García-Baonza, A. Milner, M. Paz-Pasternak, *J. Am. Chem. Soc.* **2005**, *127*, 4580–4581; d) S. M. Neville, G. J. Halder, K. W. Chapman,

M. B. Duriska, B. Moubaraki, K. S. Murray, C. J. Kepert, *J. Am. Chem. Soc.* **2009**, *131*, 12106 – 12108; e) M. Morimoto, H. Miyasaka, M. Yamashita, M. Irie, *J. Am. Chem. Soc.* **2009**, *131*, 9823 – 9835.

[2] M. Ohba, K. Yoneda, G. Agustí, M. C. Muñoz, A. B. Gaspar, J. A. Real, M. Yamasaki, H. Ando, Y. Nakao, S. Sakaki, S. Kitagawa, *Angew. Chem.* **2009**, *121*, 4861 – 4865; *Angew. Chem. Int. Ed.* **2009**, *48*, 4767 – 4771.

[3] M. Kurmoo, H. Kumagai, K. W. Chapman, C. J. Kepert, *Chem. Commun.* **2005**, 3012 – 3014.

[4] Z. M. Wang, Y. J. Zhang, T. Liu, M. Kurmoo, S. Gao, *Adv. Funct. Mater.* **2007**, *17*, 1523 – 1536.

[5] O. Sato, T. Iyoda, A. Fujishima, K. Hashimoto, *Science* **1996**, *272*, 704 – 705.

[6] a) S.-i. Ohkoshi, Y. Hamada, T. Matsuda, Y. Tsunobuchi, H. Tokoro, *Chem. Mater.* **2008**, *20*, 3048 – 3054; b) J. M. Herrera, V. Marvaud, M. Verdaguer, J. Marrot, M. Kalisz, C. Mathonière, *Angew. Chem.* **2004**, *116*, 5584 – 5587; *Angew. Chem. Int. Ed.* **2004**, *43*, 5468 – 5471; c) M. G. Hilfiger, M. Chen, T. V. Brinzari, T. M. Nocera, M. Shatruk, D. T. Petasis, J. L. Musfeldt, C. Achim, K. R. Dunbar, *Angew. Chem.* **2010**, *122*, 1452 – 1455; *Angew. Chem. Int. Ed.* **2010**, *49*, 1410 – 1413; d) C. P. Berlinguette, A. Dragulescu-Andrasi, A. Sieber, H.-U. Güdel, C. Achim, K. R. Dunbar, *J. Am. Chem. Soc.* **2005**, *127*, 6766 – 6779; e) V. Escax, G. Champion, M.-A. Arrio, M. Zacchigna, C. C. d. Moulin, A. Bleuzen, *Angew. Chem.* **2005**, *117*, 4876 – 4879; *Angew. Chem. Int. Ed.* **2005**, *44*, 4798 – 4801.

[7] A. Niemz, V. M. Rotello, *Acc. Chem. Res.* **1999**, *32*, 44 – 52.

[8] a) D. Li, R. Clérac, O. Roubeau, E. Harté, C. Mathonière, R. L. Bris, S. M. Holmes, *J. Am. Chem. Soc.* **2008**, *130*, 252 – 258; b) K. E. Funck, M. G. Hilfiger, C. P. Berlinguette, M. Shatruk, W. Wernsdorfer, K. R. Dunbar, *Inorg. Chem.* **2009**, *48*, 3438 – 3452; c) M. Shatruk, A. Dragulescu-Andrasi, K. E. Chambers, S. A. Stoian, E. L. Bominaar, C. Achim, K. R. Dunbar, *J. Am. Chem. Soc.* **2007**, *129*, 6104 – 6116; d) Y. Zhang, D. Li, R. Clérac, M. Kalisz, C. Mathonière, S. M. Holmes, *Angew. Chem.* **2010**, *122*, 3840 – 3844; *Angew. Chem. Int. Ed.* **2010**, *49*, 3752 – 3756.

[9] a) H.-R. Wen, C.-F. Wang, Y. Song, S. Gao. J.-L. Zuo, X.-Z. You, *Inorg. Chem.* **2006**, *45*, 8942 – 8949; b) R. Lescouëzec, J. Vaissermann, C. Ruiz-Pérez, F. Lloret, R. Carrsco, M. Julve, M. Verdaguer, Y. Dromzée, D. Gatteschi, W. Wernsdorfer, *Angew. Chem.* **2003**, *115*, 1521 – 1524; *Angew. Chem. Int. Ed.* **2003**, *42*, 1483 – 1486; c) L. M. Toma, R. Lescouëzec, J. Pasán, C. Ruiz-Pérez, J. Vaissermann, J. Cano, R. Carrasco, W. Wernsdorfer, F. Lloret, M. Julve, *J. Am. Chem. Soc.* **2006**, *128*, 4842 – 4853.

[10] W. Liu, H. H. Thorp, *Inorg. Chem.* **1993**, *32*, 4102 – 4105.

[11] A. L. Spek, PLATON, A Multipurpose Crystallographic Tool, Utrecht Univercity, Utrecht, The Netherlands **2001**.

[12] V. Escax, A. Bleuzen, C. Cartier dit Moulin, F. Villain, A. Goujon, F. Varret, M. J. Verdagure, *J. Am. Chem. Soc.* **2001**, *123*, 12536 – 12543.

[13] Y. Moritomo, F. Nakada, H. Kamioka, T. Hozumi, S. Ohkoshi, *Phys. Rev. B* **2007**, *75*, 214110.

[14] E. Yikilmaz, J. Xie, T. C. Brunold, A.-F. Miller, *J. Am. Chem. Soc.* **2002**, *124*, 3482 – 3483.

[15] J. Yuasa, S. Yamada, S. Fukuzumi, *Angew. Chem.* **2007**, *119*, 3623 – 3625; *Angew. Chem. Int. Ed.* **2007**, *46*, 3553 – 3555.

[16] R. Lescouëzec, J. Vaissermann, F. Lloret, M. Julve, M. Verdaguer, *Inorg. Chem.* **2002**, *41*, 5943 – 5945.

